Transient Electromagnetic Co-simulation of Electrostatic Air Discharge

Darwin Zhang Li (1), Jianchi Zhou (2), Ahmad Hosseinbeig (2), David Pommerenke (2)

(1) EMC Laboratory Missouri S&T, 4000 Enterprise Drive, Rolla, MO 6501 USA
tel.: 508-532-4312, e-mail: dzldh8@mst.edu

(2) EMC Laboratory Missouri S&T, 4000 Enterprise Drive, Rolla, MO 6501 USA

Abstract - Transient electromagnetic co-simulation is used to simulate the currents in a discharging rod. The simulation model simultaneously solves Maxwell's equation and the arc resistance equations in time domain to estimate the currents and fields for a given geometry, charge voltage and arc length. The Rompe-Weizel model is used to obtain the time dependent arc resistance, and results from different simulation methods are compared to measured data.

I. Introduction

ESD discharge between metal parts can produce discharge currents up to hundreds of ampere at sub nanosecond rise times. The current levels and rise times depend on the voltage and the local source impedance which drives the current, but also on the time dependent arc resistance which is a strong function of the arc length. The fields associated with such currents will couple into flex cables, PCBs and other metallic structures. To simulate such currents one needs to combine an electromagnetic description of the geometry with a non-linear description of the arc resistance [1]. A variety of approaches has been published such as [2],[3], and [4] which prove the concept of non-contact ESD numerical modeling and simultaneous time-stepping with SPICE, but these are only suitable for simple geometries with numerical methods that are rarely used for consumer electronics design. In this paper, we explain and compare multiple methodologies to solve for air discharge current and fields within the widely used CST Studio Suite [11]. For methodology, the full-wave simulation is either combined with the arc resistance law of Rompe-Weizel (RW) directly by exchanging voltage and current information in every time step or the combination is achieved by a two-step process which first simulates impedances which are then combined with the arc model in a circuit simulation. Using a simple model of a discharging rod, it is shown that the methodology can match measured current and current derivative results. As for the significance to system level ESD, simulation of contact mode ESD is already widely used in industry to predict results such as soft failures [12], and we will analyze how this new methodology can improve the existing simulation workflows with a simple real world example with an ESD gun.

II. Measurement Techniques

The experimental setup is similar to the one used in [1].

A. Measurement Equipment

Figure 1 shows the test setup. A 102 cm long rod with 1.80 cm diameter placed above ground forms a transmission line impedance of about 200 ohm characteristic impedance.

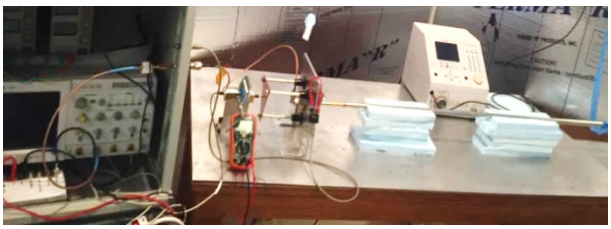

Figure 1: Test setup showing the rod, arc length measurement, oscilloscope in a shielded enclosure and the high voltage supply inside a climate chamber.

The tip of the rod is round. The diameter reduces from 1.8cm to 1.35 cm close to the discharge point as shown on the transition on the rod in Figure 2.

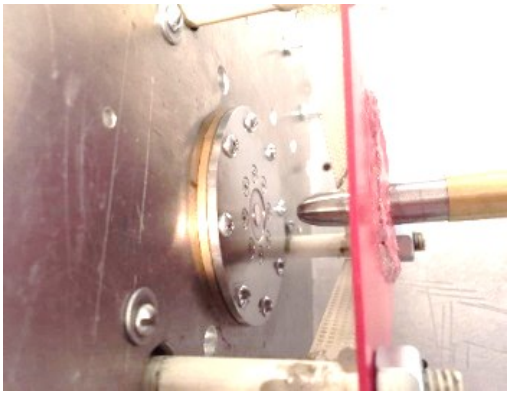

Figure 2: Rod Tip and parts of the arc length measurement system

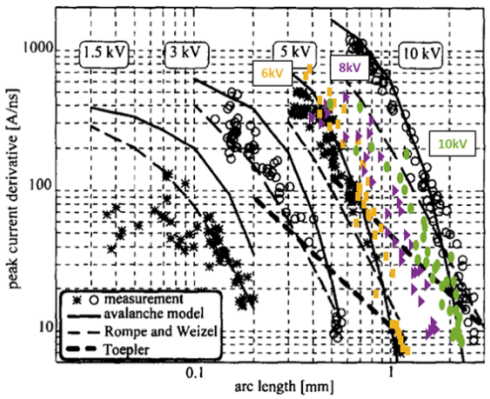

Figure 3: Peak Derivative Current measurement results at 22% Humidity and 15ºC overlaid on the results published in [1]

B. Measurement Procedure

The rod is charged to 6, 8, or 10 kV and moved towards the ESD current target. Once a discharge event occurs, the arc length is measured and the current is recorded. For slow approach speeds, the arc length will equal the value predicted by Paschen's Law. For faster approach speeds, the arc length is reduced due to the interplay of the statistical time lag [5] and the speed of approach. For the purposes of the measurement procedure, "slower" and "faster" approach speeds are only qualitative and there was no measurement made on the actual speed the experimenter's hand moved. Qualitative approach speed is confirmed to be sufficient since the experimenter was able to collect a good range of raw data to view in Figure 3. The setup of this equipment and data collection is explained in detail in [1].

C. Measurement Results

Figure 3 presents measured results for the peak current derivative and compares them to published data [1] of a related, but not identical geometry. The comparison indicates a general agreement which gives confidence in the measured data. Furthermore, this also gives confidence in the basic underlying arc resistance law.

III. Simulation Technique

A. Simulation Modeling

Four different simulation models and methods are used. Z-Parameters used here is synonymous with Impedance Parameters, which are defined as a matrix of N by N size solved by $V_m = [Z_{m,n}]I_n$ for an N port network where V_m and I_n are the Voltages and Currents at port m and n respectively. Z-Parameters may be transformed into S-parameters and vice-versa.

a) The rod model's impedance between the end of the rod and the ESD target is simulated in frequency domain using Finite Element Method (FEM). The impedance information (Z-parameters) is compared to the other simulation algorithms (Figure 6)

b) The same is done with the Finite Integration Technique (FIT) for Figure 6.

c) The same above is done with Transmission Line Matrix (TLM) for Figure 6, but in addition to it, the Z-Parameters, expressed as S-parameters is used in a SPICE-like simulation after combining it with the arc resistance model. This produces the results in Figure 9.

d) A transient co-simulation is performed. During the transient co-simulation, the arc resistance model is directly attached to the 3D structure. During each time step voltage and current information is exchanged between the arc resistance model and the electromagnetic simulation. For the transient co-simulation the voltage and arc length must be given prior to starting the simulation.

Figure 4 depicts the CST Microwave Studio simulation model. The ports in the 3D modeler connect to the circuit simulator which allows for modeling non-linear elements such as SPICE models.

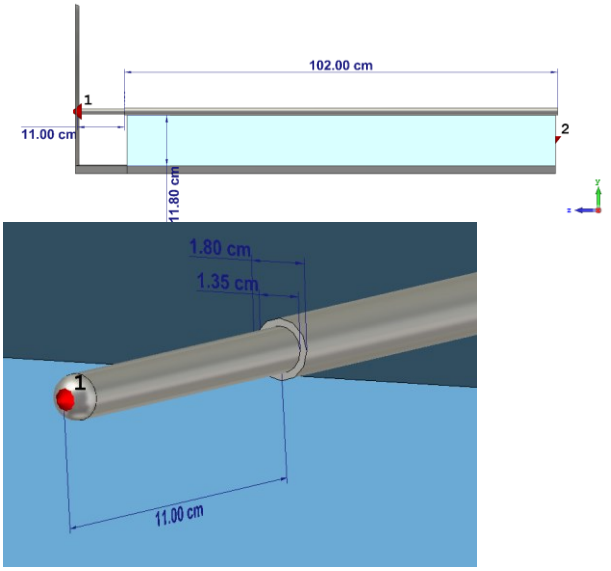

Figure 4: Rod with round tip discharging to a ground plane. Labels 1 and 2 are the ports

Figure 5 shows the different meshing schemes. It is apparent that the sub-gridding utilized by the TLM mesh is the most efficient grid solution. It avoids gridding regions that do not need fine grid (grid bleeding) seen in the FIT grid. The TLM solution is obtained in 25 minutes vs. 45 minutes in FIT. Experience in comparing TLM to FIT solution has shown that the optimal solution is problem dependent, however discussing the underlying reason is beyond the scope of this paper. Neither method shows consistent advantage over the other gridding method. As the TLM solution offered faster solution speed it was used in most of the simulations presented here.

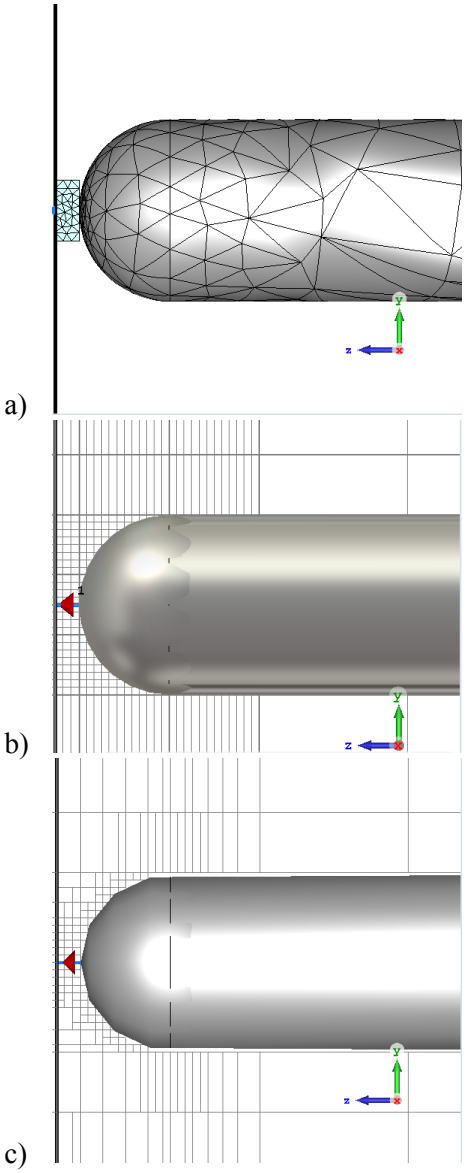

Figure 5: Different meshing algorithms. From Top to Bottom: a) FEM, b) FIT, and c) TLM

Since transient-co-simulation requires a time-domain algorithm to simultaneously pass the voltages and currents between the 3D full-wave model and the non-linear circuit elements, FEM cannot be used to obtain non-linear time domain results directly. Nevertheless, it is good to run with FEM at least to show the agreement of the Z-Parameters at low frequency as shown in Figure 6.

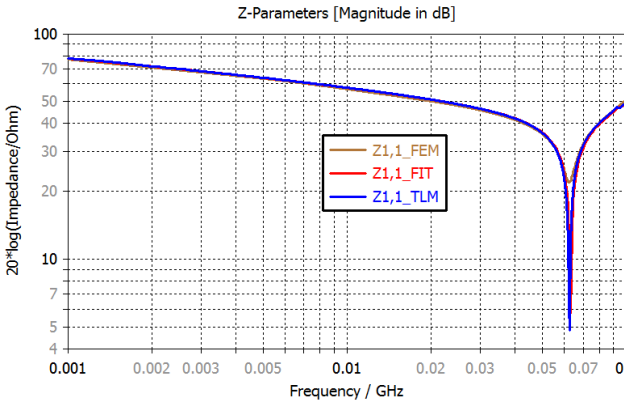

Figure 6: Z-Parameters comparison for the impedance between the tip of the rod and ground for three full-wave algorithms

Figure 7 shows the circuit modeler in CST that integrates the 3D Model and the circuit elements.

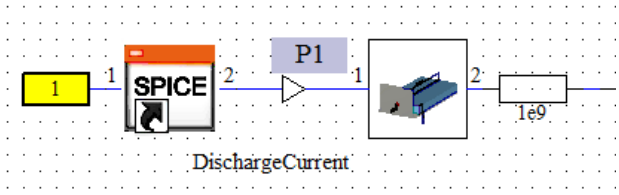

Figure 7: Circuit setup in CST Design Studio with Port 1 connecting to the Rompe-Weizel spice mode, a probe to monitor the current at P1, the connection to the 3D Rod model's port placed at the rod's tip, and a large value termination resistor connected to the other port at the rod in its 3D representation

At Port 1, the same input voltage waveform is used as [7][8], which is a high voltage. The Rompe-Weizel model (abbreviated as RW) describes the time-dependent arc resistance [1]:

$$R(t) = d \Big/ \sqrt{2 \cdot a \cdot \int_0^t i(x)^2 dx}$$

Where $\boldsymbol{R}$ is the arc resistance in Ohms, $\boldsymbol{d}$ is the gap distance of the electrode or arc length in meters and will be swept for different values in simulation. $\boldsymbol{a}$ is an empirical constant with value of $1.5e-4\ \frac{m^2}{V^2 \cdot s}$ and i is the discharge current in amperes.

The SPICE code for the RW model is given in [8] and was adapted to be compatible with CST. There are two methods presented in this paper to run the simulation with this SPICE Model. The first method presented in this paper is a two-step process for obtaining currents:

1) The structure is simulated using a 3D solver (time or frequency domain). This 3D analysis provides the full S Matrix.
2) The S Matrix is used in the circuit simulator for further tasks such as finding the response to the RW model.

This two-step process is not complete with regards to field results. The method and results from [7] show that it is possible to take the currents from the two-step process and then re-import them into CST as a custom waveform to get the transient fields. However, this method of re-import is not generalizable to other Rompe-Weizel model applications such as secondary air discharge, which depends heavily on voltages at the gap [9]. Furthermore, the re-import method still requires two simulations. The second method presented in this paper, which is transient co-simulation, requires only one simulation and does not require a re-import. As explained below, Transient co-simulation is complete and essential for ESD simulation and visualization of surface currents in time due to the ESD event. Transient-co-simulation is used with 3D transient solvers (FIT or TLM) and time stepping is performed on the circuit and 3D level simultaneously. This then allows field visualization with included non-linear elements in the 3D simulation.

B. Simulation Results

1. Comparing Current Waveforms

It is not possible to match the current waveforms exactly to measurement, but for ESD induced soft-failure, mainly the peak current and current rise time are the results of interest. As shown in Figure 8, the simulated current waveforms have the correct features which include the peak discharge current.

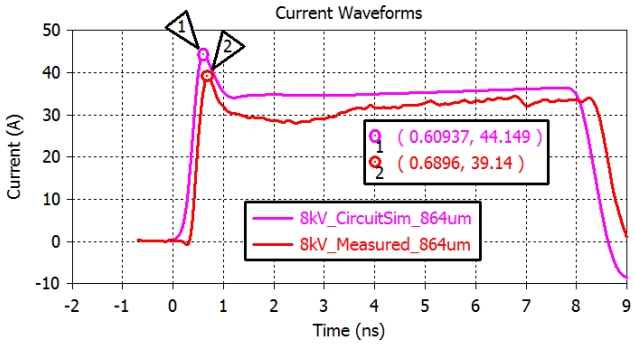

Figure 8: Comparison of the Current Waveform with the peaks

After the first peak one needs to consider that the RW model leads to a very low resistance and a low voltage drop along the arc. However, the real arc may act more like a constant voltage drop of 25-40V. At present, we did not include this transition from a resistive phase to a constant voltage drop phase into the modeling.

2. Comparing Simulation to Measurement

Arc length ***d*** in the SPICE file is swept at 0.1 mm to simulate the max(di/dt) vs. arc length at step 2) of the two-step process. We treat arc length as being the same as the gap distance between the tip of the rod and the ground plane. We are interested in max(di/dt) vs. arc length because rate of current change and the associated rise time are important with respect to induced noise voltages. This comparison is shown in Figure 9. Since the measurement data is bandwidth limited by the oscilloscope, a 3 GHz filter with rectangular response is applied:

$$H(f) = \begin{cases} 1, & f < 3\ GHz \\ 0, & f \geq 3GHz \end{cases}$$

The following steps are taken to apply the filter:

1) Obtain the current waveform (Simulation)
2) Fourier Transform (Post-Processing)
3) Apply the above low pass filter (Post-Processing)
4) Inverse Fourier Transform (Post-Processing)
5) Compute max(di/dt) (Post-Processing)

The results shown in Figure 9 present the measured data and the simulation. The simulation data is shown as functions relating the max(di/dt) to the arc length. The measurement data is presented as one value per measurement performed. Both measured and simulated data show an increase of the max(di/dt) if the arc length is reduced. However, this increase levels off. The leveling off is a result of the measurement bandwidth and can be matched by simulation if a 3 GHz low pass filter is applied. Each of the voltage levels has distinct results, which is the correct behavior that implies repeatability [1]. For the transient co-simulation, it is swept at 0.2 mm intervals but the results are exactly the same as the two-step process.

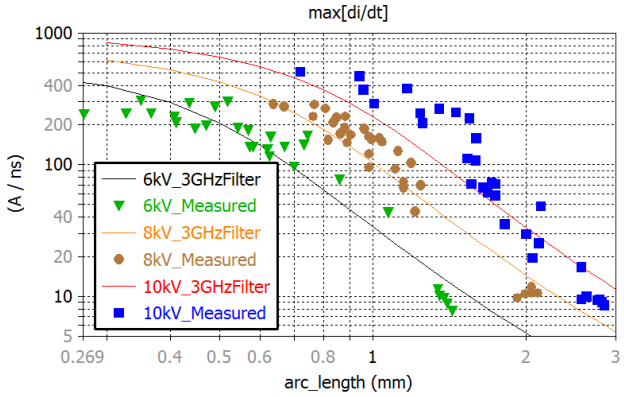

Figure 9: Comparison of maximum time derivative of current between Simulation and Measurement

For this study, the two-step process requires a single 25 minute run for S-Parameters and then a few seconds for each circuit simulator run. Transient co-simulation takes 1 hour for each run, but since transient co-simulation is the only way to get transient Field data, then this would be the method for completeness. Furthermore, numerical convergence of the discharge current is guaranteed with transient co-simulation whereas the two-step process requires convergence at step 1) for the S matrix.

3. Simple example with realistic ESD generator

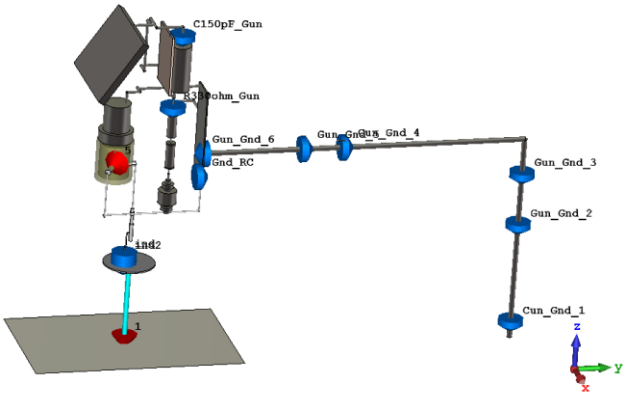

Figure 10: Example model of a ESD Generator discharging to a metal plane in non-contact/air gap mode (0.8 mm gap distance and 8 kV)

As mentioned in international ESD testing standard IEC 61000-4-2 [13], ESD current has a wide frequency bandwidth and a high peak current level which can cause failures in the device. An ESD air-gap discharge testing scenario can be modeled

with a realistic ESD generator and a DUT. Many references have already shown that this can be done with simulation even for today's ESD generators used in the industry in contact mode [6][10][12]. In particular the work in [10] is relevant to the modeling and simulation of such generators. The only change that would need to be made from using the methodology of [10] is that a port can then go in between the ESD gun tip and ground plane rather than a lumped element to facilitate the interfacing between full-wave and circuit that includes the Rompe-Weizel SPICE model. As shown in Figure 10, a complex ESD generator is modeled in full-wave and discharging to a ground plane. The current distribution in 3D is given in Figure 12 at three different times and highlights the novelty in this new methodology of a single transient co-simulation for system-level considerations. In Figure 11, the current waveform can be seen at the air-gap and can be correlated to Figure 12. Just as we expect from looking at Figure 11, there is negligible current that forms on the ground plane until 1.5 ns, and this is what we see from looking at the plots of Figure 12 in that order.

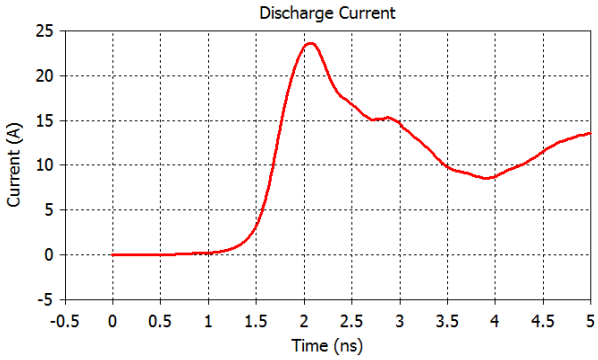

Figure 11: Current waveform from the arc across the air gap for the example in Figure 10.

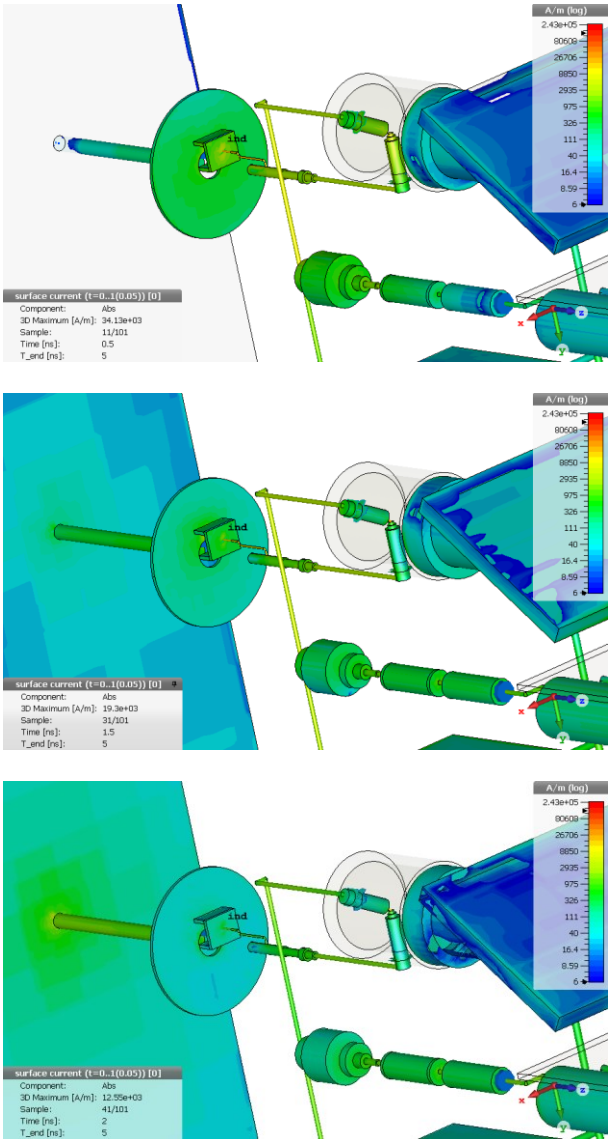

Figure 12: Surface current plots at 0.5 ns, 1.5 ns, and 2.0 ns for the example in Figure 10.

4. Extensions

The paper describes a methodology that allows design engineers to make decisions on mechanical design related to ESD system level performance. For example, if the industrial design engineer suggests a decorative metal which is not electrically connected to the local ground of the device under test, then a secondary ESD event is possible. The simulation methodology will be able to predict the discharge currents of such secondary ESD as a function of the gap length and capacitance of the decorative method. With

increasing capacitance the secondary ESD current will rapidly increase, and this can be quantified by the simulation methodology. Using the simulated secondary ESD currents, the coupling into the electronics can be simulated and one can determine how much additional shielding is needed to compensate for the effect of an increased decorative metal part. Such a simulation may indicate that a two-layer flex cable may be needed if a larger decorative metal is used to avoid additional coupling to the signals on the flex cable.

Acknowledgment

This material is based upon work supported by the National Science Foundation (NSF) under Grants IIP-1440110.

Conclusion

A measurement setup that is well known in literature [1] is used and a full-wave simulation of this setup is accomplished. Analysis of different numerical methods leads to the conclusion that for this particular measurement setup, the TLM algorithm has the best performance, and the two-step process is used to gather the current waveforms and rise times. Transient co-simulation, which is a new method for air gap discharge with the Rompe-Weizel model, is presented and its ability of complete transient field data all in one simulation run is compared to the two-step process and the re-import method of [7]. Simulation results correlate very well to the measurement which shows the validity of the numerical methods used. Finally, results from a simple example with a realistic ESD generator discharging to a ground plane are shown.

References

[1] David Pommerenke, ESD: Transient fields, arc simulation and rise time limit, Journal of Electrostatics, Volume 36, Issue 1, 1995, Pages 31-54, ISSN 0304-3886

[2] R. Jobava et al., "Computer simulation of ESD from cone," Proceedings of III International Seminar/Workshop on Direct and Inverse Problems of Electromagnetic and Acoustic Wave Theory. (IEEE Cat. No.98EX163), Tbilisi, 1998, pp. 111-113.

[3] K. Fujita and T. Namiki, "FDTD-SPICE direct linking simulation of transient fields caused by electrostatic discharge," 2013 International Symposium on Electromagnetic Theory, Hiroshima, 2013, pp. 112-115.

[4] K. Fujita, J. Zhou and D. Pommerenke, "Hybrid full-wave/circuit modelling of spark gaps and its experimental validation," in Electronics Letters, vol. 53, no. 7, pp. 484-486, 3 30 2017

[5] F. Wan, V. Pilla, J. Li, D. Pommerenke, H. Shumiya and K. Araki, "Time Lag of Secondary ESD in Millimeter-Size Spark Gaps," in IEEE Transactions on Electromagnetic Compatibility, vol. 56, no. 1, pp. 28-34, Feb. 2014.

[6] S. Caniggia and F. Maradei, "Numerical Prediction and Measurement of ESD Radiated Fields by Free-Space Field Sensors," in IEEE Transactions on Electromagnetic Compatibility, vol. 49, no. 3, pp. 494-503, Aug. 2007

[7] D. Liu et al., "Full-Wave Simulation of an Electrostatic Discharge Generator Discharging in Air-Discharge Mode Into a Product," in IEEE Transactions on Electromagnetic Compatibility, vol. 53, no. 1, pp. 28-37, Feb. 2011.

[8] David Pommerenke, Martin Aidam, ESD: waveform calculation, field and current of human and simulator ESD, Journal of Electrostatics, 38(1-2):33-51, October 1996

[9] H. Wolf and H. Gieser, "Secondary discharge - A potential risk during system level ESD testing," 2015 37th Electrical Overstress/Electrostatic Discharge Symposium (EOS/ESD), Reno, NV, 2015, pp. 1-7.

[10] D. Liu, A. Nandy, D. Pommerenke, S. J. Kwon and K. H. Kim, "Full wave model for simulating a Noiseken ESD generator," 2009 IEEE International Symposium on Electromagnetic Compatibility, Austin, TX, 2009, pp. 334-33

[11] CST (Computer Simulation Technology) Microwave Studio version 2017: https://www.cst.com/

[12] K. H. Kim, J. H. Koo, B. G. Kang, S. J. Kwon, Y. Kim and J. Jeong, "Systematic

design technique for improvements of mobile phone's immunity to electrostatic discharge soft failures," 2010 IEEE International Symposium on Electromagnetic Compatibility, Fort Lauderdale, FL, 2010, pp. 348-353.

[13] EMC—Part 4-2: Testing and Measurement Techniques—Electrostatic Discharge Immunity Test, Int. Electrotech. Commiss. (IEC), Geneva, Switzerland, IEC 61000-4-2 International Standard, 2001